Bernoulli free boundary problems under uncertainty: the convex case

M. Dambrine, H. Harbrecht, B. Puig

Departement Mathematik und Informatik
Fachbereich Mathematik
Universität Basel
CH-4051 Basel

Preprint No. 2022-04
February 2022

dmi.unibas.ch

Bernoulli free boundary problems under uncertainty: the convex case

M. Dambrine, H. Harbrecht and B. Puig

February 11, 2022

Abstract

The present article is concerned with solving Bernoulli's exterior free boundary problem in case of an interior boundary which is random. We provide a new regularity result on the map that sends a parametrization of the inner boundary to a parametrization of the outer boundary. Moreover, by assuming that the interior boundary is convex, also the exterior boundary is convex, which enables to identify the boundaries with support functions and to determine their expectations. We in particular construct a confidence region for the outer boundary based on Aumann's expectation and provide a numerical method to compute it.

1 Introduction

The subject of shape optimization under uncertainties has emerged in recent years. The first approaches in the literature are based on linearization with respect to random input parameters. Such a linearization is justified when the uncertainties are assumed to be small. Then, one might either optimize the objective under consideration under a worst case point of view (see the seminal work of Allaire and Dapogny [4]) or one optimizes an averaged version of the objective (see our work [9] and those of Allaire and Dapogny [5]), provided that some statistical data is given on the uncertain parameters at hand. All these works have been dealing with problems in optimization of elastic structures, where the optimization criteria were clearly motivated from an engineering point of view.

Fewer works have considered problems where a shape is the unknown and where shape optimization is then a convenient reformulation of the problem. This is the case in inverse (shape identification) problems and in free boundary problems. In the case of inverse problems, we have proposed in [10] a strategy which is based on the minimization of an averaged version of the objective, possibly modified by moments of its distribution. However, those reconstructions depend on the criterion selected to achieve the reconstruction. This is a non-intrinsic choice of the solution strategy and it seems to us more natural to tackle the random inverse problem in the converse point of view: solve the problem for each realization of the parameters and then average it. Of course, when studying practical inverse problems, one has in general no uniqueness of the solution or only weak stability of the reconstruction. Therefore, we focus in this work on a free boundary problem, where we can follow the strategy first solve the free boundary and then average it. This program requires to investigate the field of random sets.

We have presented in [11, 15] the first numerical study of random free boundary problems, where we discussed the notion of the expected free boundary that makes sense and its practical computation. In

the present work, we want to go one step further: we are interested in providing numerical confidence intervals (i.e. regions in this geometrical context) for the free boundary. Notice that there are only very few works about this topic in the literature (see [8] for the case of convex random sets and [12, 18] for oriented distance based random sets). In our previous work [12], we proposed some semi-analytical computations in the context of the oriented distance based expectation. However, the computational cost of the confidence interval was unfeasible except for elementary examples.

In order to work on a well-founded theoretical fundament and to obtain tractable numerical simulations, we restrict this study to the case of Bernoulli's exterior free boundary problem when the data (the inner boundary) is the boundary of a random convex compact set. Indeed, working with convex sets allows to use a rather intrinsic notion of expectation – the Aumann expectation. It is based on the support function and has nice properties with respect to Hausdorff distance between sets. Moreover, under the convexity assumption, the free boundary problem is known to admit a unique solution.

The contribution of this work is twofold. First, we provide, in the context of convex sets, *a regularity result (Theorem 2.3) for the map that sends a parametrization of the inner boundary to a parametrization of the outer one.* This result is established in the deterministic setting, but partially explains why a "nice" distribution of the inner boundary generates a "nice" distribution of the outer boundary, which enables the computation of an average of the outer boundary. The proof of this result is based on the implicit function theorem applied to Trefftz's formulation of a nonlinear system of integral equations for computing the free boundary. Second, we *propose a numerical method in order to compute an asymptotic confidence region for the outer boundary by using Aumann's expectation.* Our theoretical findings are supported by numerical illustrations.

The rest of this work is structured as follows. In Section 2, we present the exterior Bernoulli free boundary, define the Bernoulli map that sends the inner boundary to the outer one, state our regularity result, and finally prove it. Then, in Section 3, we gather deep results on random convex compact sets. In particular, we present the Aumann expectation of random convex compact sets and its connection to the support function of these sets. We quote the corresponding central limit theorem and we derive the associated result on the asymptotic confidence region. We then present in Section 4 the numerical method we use to compute a specific random sample, i.e., to solve a (deterministic) Bernoulli free boundary problem. It is the so-called trial method which is realized by using a reformulation of the underlying Laplace problem by means of a boundary integral equation. We also explain how to compute the asymptotic confidence region by a using a bootstrapping method. Finally, we present numerical studies for two random free boundary problems in Section 5.

2 The exterior Bernoulli free boundary problem

Let K be a compact regular domain in $\mathbb{R}^d$ ($d = 2, 3$) and let λ a positive real number. The problem of finding a domain D and a function u such that the capacity potential of K in D defined as the solution of

$$\left\{ \begin{array}{rcll} -\Delta u & = & 0 & \text{in } D \setminus K \\ u & = & 1 & \text{on } \partial K = \Sigma \\ u & = & 0 & \text{on } \partial D = \Gamma \end{array} \right. \tag{2.1}$$

satisfies the overdetermination condition

$$|\nabla u| = \lambda \text{ on } \Gamma \tag{2.2}$$

is called the exterior Bernoulli free boundary problem. Notice that this overdetermination condition means that for any $x \in \Gamma$

$$\lim_{y \in D,\, y \to x} |\nabla u(y)| = \lambda.$$

For general compact sets K, there may exist more than one solution to the free boundary value problem. Nevertheless, there are classes of compact sets K such that the free boundary problem admits a unique solution. The largest one is the class of starlike domains [24]. An interesting subclass of starlike domains is the one of convex domains. For convex domains, the free boundary problem admits exactly one solution (D, u) and moreover, in [17, Theorem 2-1], Henrot and Shahgholian proved that the domain D is convex if K is.

We shall therefore introduce $\mathcal{S}$ as the space of starlike domains in $\mathbb{R}^d$ and $\mathcal{K}$ as the space of convex compact subsets of $\mathbb{R}^d$. The generalization of the result of Henrot and Shahgholian allows us to define the Bernoulli map $\mathcal{B} : \mathcal{K} \times (0, \infty) \to \mathcal{K}$ which sends a convex compact set $K \in \mathcal{K}$ and a value $\lambda \in (0, \infty)$ to the closure of the unique domain D that is the solution of the exterior Bernoulli free boundary problem (2.1).

2.1 Regularity of the Bernoulli map $\mathcal{B}$

We shall next describe the properties of the mapping $\mathcal{B}$. This study was mainly performed by Hayouni, Henrot and Samouh in [16]. Let us first present the monotonicity properties of the map by gathering results of [16] for the continuity properties and by extending ideas of [20] for the differentiability properties.

Theorem 2.1 (Monotonicity of the map) *The map $\mathcal{B} : \mathcal{K} \times (0, \infty) \to \mathcal{K}$ is*

1. *non-decreasing with respect to inclusion: Let K_1 and K_2 be two compact sets with $K_1 \subset K_2$. Then, for any $\lambda > 0$, $\mathcal{B}(K_1, \lambda) \subset \mathcal{B}(K_2, \lambda)$;*

2. *decreasing with respect to the constant: Let λ_1 and λ_2 be two nonnegative real numbers with $\lambda_1 < \lambda_2$. Then, for any K, $\mathcal{B}(K, \lambda_2) \subset \mathcal{B}(K, \lambda_1)$ with $\mathcal{B}(K, \lambda_2) \neq \mathcal{B}(K, \lambda_1)$.*

We are now interested in the regularity of the mapping $\mathcal{B}$. To this end, we first recall the continuity result of Henrot and the properties of the application of $\mathcal{B}$ gathering results from [16, Theorems 2-2 and 3-1].

Proposition 2.2 (Properties of the map) *The map $\mathcal{B} : \mathcal{K} \times (0, \infty) \to \mathcal{K}$ is continuous.*

Indeed, in the convex case, there is even more regularity. However, this regularity cannot be obtained through the Hausdorff distance and the support function parametrization. The idea is to define parametrizations of the inner boundary $\Sigma = \partial K$ and of the outer boundary $\Gamma = \partial D$. Since a convex set is also starlike, we can represent the unknown boundaries Σ and Γ with the help of radial functions according to

$$\begin{array}{rcl} \boldsymbol{\sigma} & : & \mathbb{S}^1 \to \Sigma, \\ & & \boldsymbol{\sigma}(\varphi) = r_\Sigma(\varphi)\mathbf{e}_r(\varphi); \end{array} \qquad \begin{array}{rcl} \boldsymbol{\gamma} & : & \mathbb{S}^1 \to \Gamma, \\ & & \boldsymbol{\gamma}(\varphi) = r_\Gamma(\varphi)\mathbf{e}_r(\varphi). \end{array}$$

We make in addition the assumption that both $\boldsymbol{\gamma}$ and $\boldsymbol{\sigma}$ are $\mathcal{C}^k$ for some integer $k \geq 2$. We are now in position to state our main theoretical result.

Theorem 2.3 *The map $\widetilde{\mathcal{B}}$, defined from $\mathcal{C}^k(\mathbb{S}^1)$ with values in $\mathcal{C}^k(\mathbb{S}^1)$ such that $\widetilde{\mathcal{B}}(\boldsymbol{\sigma})$ is the polar parametrization of the solution to Bernoulli's free boundary problem associated to the inner boundary $\Sigma = \boldsymbol{\sigma}(\mathbb{S}^1)$, is $\mathcal{C}^{k-1}$ around each $\boldsymbol{\sigma}$ such that Σ is convex. Its restriction to $\mathcal{C}^\infty(\mathbb{S}^1)$ is $\mathcal{C}^\infty$.*

The proof of this theorem is inspired by the work of Kress in [20, 27] where he introduced a new numerical method in order to approximate the solution of Bernoulli's free boundary problem. The key idea of Kress is to use the integral equation point of view to solve Dirichlet boundary value problems and to solve Bernoulli's free boundary problem by Trefftz's method. We will present the proof in the case $d = 2$. The extension to the case $d \geq 3$ is similar (see the differences between [20] and [27] in order to extend the proof from $d = 2$ and $d = 3$).

2.2 Proof of Theorem 2.3

Let us recall the definition of the object we shall use. Consider G to be the Green function for the Laplacian that is given in two spatial dimensions by

$$G(\mathbf{x}, \mathbf{y}) = -\frac{1}{2\pi} \log \|\mathbf{x} - \mathbf{y}\|_2.$$

Namely, the solution $u(\mathbf{x})$ of (4.1) is given in each point $\mathbf{x} \in D \setminus K$ by Green's representation formula

$$u(\mathbf{x}) = \int_{\Gamma \cup \Sigma} \left\{ G(\mathbf{x}, \mathbf{y}) \frac{\partial u}{\partial \mathbf{n}}(\mathbf{y}) - \frac{\partial G(\mathbf{x}, \mathbf{y})}{\partial \mathbf{n}_\mathbf{y}} u(\mathbf{y}) \right\} \mathrm{d}\varsigma_\mathbf{y}. \tag{2.3}$$

Using the jump properties of the layer potentials, we obtain the direct boundary integral formulation of the problem

$$\frac{1}{2} u(\mathbf{x}) = \int_{\Gamma \cup \Sigma} G(\mathbf{x}, \mathbf{y}) \frac{\partial u}{\partial \mathbf{n}}(\mathbf{y}) \mathrm{d}\varsigma_\mathbf{y} - \int_{\Gamma \cup \Sigma} \frac{\partial G(\mathbf{x}, \mathbf{y})}{\partial \mathbf{n}_\mathbf{y}} u(\mathbf{y}) \mathrm{d}\varsigma_\mathbf{y}, \tag{2.4}$$

where $\mathbf{x} \in \Gamma \cup \Sigma$. If we label the boundaries by $A, B \in \{\Gamma, \Sigma\}$, then (2.4) includes the single layer operator

$$\mathcal{V}_{AB} : \mathcal{C}(B) \to \mathcal{C}(A), \quad \big(\mathcal{V}_{AB}\rho\big)(\mathbf{x}) = -\frac{1}{2\pi} \int_B \log \|\mathbf{x} - \mathbf{y}\|_2 \, \rho(\mathbf{y}) \mathrm{d}\varsigma_\mathbf{y} \tag{2.5}$$

and the double layer operator

$$\mathcal{K}_{AB} : \mathcal{C}(B) \to \mathcal{C}(A), \quad \big(\mathcal{K}_{AB}\rho\big)(\mathbf{x}) = \frac{1}{2\pi} \int_B \frac{\langle \mathbf{x} - \mathbf{y}, \mathbf{n}_\mathbf{y} \rangle}{\|\mathbf{x} - \mathbf{y}\|_2^2} \rho(\mathbf{y}) \mathrm{d}\varsigma_\mathbf{y} \tag{2.6}$$

with the densities $\rho \in \mathcal{C}(A)$ being the Neumann data of u on A.

Step 1: Reformulation as a system of integral equations. The first step is [20, Theorem 1]: solving Bernoulli's free boundary is equivalent to solving the nonlinear system of integral equation

$$\begin{aligned} -\lambda \mathcal{V}_{\Gamma\Gamma}\, 1 + \mathcal{V}_{\Gamma\Sigma}\, g &= 0, \\ -\lambda \mathcal{V}_{\Sigma\Gamma}\, 1 + \mathcal{V}_{\Sigma\Sigma}\, g &= 1, \end{aligned} \tag{2.7}$$

for the unknowns D and $g = \partial_n u$ on $\partial K = \Sigma$. We first define the parametrized single layer operators

$$S_{AB} : \mathrm{H}^{-1/2}(\mathbb{S}^1) \to \mathrm{H}^{1/2}(\mathbb{S}^1)$$

such that $(\mathcal{V}_{AB}\varphi)\circ z_A = S_{AB}(\varphi\circ z_B)$, where $A,B\in\{\Sigma,\Gamma\}$ and likewise $z_\Sigma=\boldsymbol{\sigma}$. Hence, we have

$$(S_{AB}\,u)(t) = -\frac{1}{2\pi}\int_0^{2\pi} \ln\|z_A(t)-z_B(\tau)\|\,\|z_B'(\tau)\|\,u(\tau)\,\mathrm{d}\tau$$

for all $t\in[0,2\pi)$. Notice that the operator $S_{\Sigma\Sigma}$ does not depend on $\boldsymbol{\gamma}$ while $S_{\Sigma\Gamma}$, $S_{\Gamma\Gamma}$ and $S_{\Gamma\Sigma}$ do. Likewise, $S_{\Gamma\Gamma}$ does not depend on $\boldsymbol{\sigma}$ while $S_{\Gamma\Sigma}$, $S_{\Sigma\Sigma}$ and $S_{\Sigma\Gamma}$ do. To emphasize this dependency, we will use the notations $S_{\Gamma\Gamma}[\boldsymbol{\gamma}]$, $S_{\Sigma\Sigma}[\boldsymbol{\sigma}]$, $S_{\Sigma\Gamma}[\boldsymbol{\gamma},\boldsymbol{\sigma}]$ and $S_{\Gamma\Sigma}[\boldsymbol{\gamma},\boldsymbol{\sigma}]$.

Step 2: Introducing the application of the implicit function theorem. We define the map

$$F : \mathcal{C}^k(\mathbb{S}^1)\times\mathcal{C}^k(\mathbb{S}^1)\times\mathrm{H}^{-1/2}(\mathbb{S}^1)\longrightarrow\mathrm{H}^{1/2}(\mathbb{S}^1)\times\mathrm{H}^{-1/2}(\mathbb{S}^1)$$

by

$$F\left(\boldsymbol{\gamma},\boldsymbol{\sigma},g\right) = \left(-\lambda S_{\Gamma\Gamma}[\boldsymbol{\gamma}]1 + S_{\Gamma\Sigma}[\boldsymbol{\gamma},\boldsymbol{\sigma}]g, -\lambda S_{\Sigma\Gamma}[\boldsymbol{\gamma},\boldsymbol{\sigma}]1 + S_{\Sigma\Sigma}[\boldsymbol{\sigma}]g\right)$$

such that the system (2.7) of integral equations is equivalent to the nonlinear equation

$$F\left(\boldsymbol{\gamma},\boldsymbol{\sigma},g\right) = (0,1)\,.$$

We shall apply the implicit function theorem to this equation around any particular solution $(\boldsymbol{\gamma}_0,\boldsymbol{\sigma}_0,g_0)$ of the previous solution. Let u_0 be the solution of (2.1) associated to the data $(\boldsymbol{\gamma}_0,\boldsymbol{\sigma}_0,g_0)$. By construction, its normal derivative $g=\partial_{\mathbf{n}}u_0$ on Σ_0 satisfies $g_0 = g\circ\boldsymbol{\sigma}$. Since F is linear in g, its regularity is limited by its partial regularity with respect to $\boldsymbol{\gamma}$ and $\boldsymbol{\sigma}$. Nonetheless, in the following, we only need to consider the derivatives with respect to g and $\boldsymbol{\sigma}$, and not with respect to $\boldsymbol{\gamma}$.

Step 3: Computing the partial derivatives. The Fréchet derivatives of the integral operators S_{AB} are obtained by differentiating their kernels with respect to $\boldsymbol{\gamma}$ (see [19, Section 18.3] for the general proof and [20] for its adaptation to the case of Sobolev spaces). Therefore, F is $\mathcal{C}^{k-1}$ and its partial derivative with respect to $(\boldsymbol{\sigma},g)$ is given by

$$D_{\boldsymbol{\sigma},g}F(\boldsymbol{\gamma}_0,\boldsymbol{\sigma}_0,g_0).[\boldsymbol{\xi},h] = \begin{pmatrix} -D_{\boldsymbol{\sigma}}S_{\Gamma\Sigma}[\boldsymbol{\gamma}_0,\boldsymbol{\sigma}_0].\boldsymbol{\xi}\,g_0 + S_{\Gamma\Sigma}[\boldsymbol{\gamma}_0,\boldsymbol{\sigma}_0]\,h \\ -\lambda D_{\boldsymbol{\sigma}}S_{\Sigma\Gamma}[\boldsymbol{\gamma}_0,\boldsymbol{\sigma}_0].\boldsymbol{\xi}\,1 + D_{\boldsymbol{\sigma}}S_{\Sigma\Sigma}[\boldsymbol{\sigma}_0].\boldsymbol{\xi}\,g_0 + S_{\Sigma\Sigma}[\boldsymbol{\gamma}_0,\boldsymbol{\sigma}_0]\,h \end{pmatrix}.$$

Here, the derivatives of the single layer operators with respect to $\boldsymbol{\sigma}$ are

$$D_{\boldsymbol{\sigma}}S_{\Sigma\Sigma}[\boldsymbol{\gamma}_0,\boldsymbol{\sigma}_0].\boldsymbol{\xi}\;u(t) = \frac{1}{2\pi}\int_0^{2\pi}\frac{[\boldsymbol{\sigma}(t)-\boldsymbol{\sigma}(\tau)]\cdot[\boldsymbol{\xi}(\tau)-\boldsymbol{\xi}(t)]}{\|\boldsymbol{\sigma}(t)-\boldsymbol{\sigma}(\tau)\|^2}\|\boldsymbol{\sigma}'(\tau)\|\,u(\tau)\,\mathrm{d}\tau + S_{\Sigma\Sigma}\left(u\,\frac{\boldsymbol{\sigma}'\cdot\boldsymbol{\xi}'}{\|\boldsymbol{\sigma}'\|^2}\right)(t),$$

$$D_{\boldsymbol{\sigma}}S_{\Gamma\Sigma}[\boldsymbol{\gamma}_0,\boldsymbol{\sigma}_0].\boldsymbol{\xi}\;u(t) = \frac{1}{2\pi}\int_0^{2\pi}\frac{[\boldsymbol{\gamma}(t)-\boldsymbol{\sigma}(\tau)]\cdot\boldsymbol{\xi}(t)}{\|\boldsymbol{\gamma}(t)-\boldsymbol{\sigma}(\tau)\|^2}\|\boldsymbol{\sigma}'(\tau)\|\,u(\tau)\,\mathrm{d}\tau + S_{\Gamma\Sigma}\left(u\,\frac{\boldsymbol{\sigma}'\cdot\boldsymbol{\xi}'}{\|\boldsymbol{\sigma}'\|^2}\right)(t),$$

and

$$D_{\boldsymbol{\sigma}}S_{\Sigma\Gamma}[\boldsymbol{\gamma}_0,\boldsymbol{\sigma}_0].\boldsymbol{\xi}\;u(t) = -\frac{1}{2\pi}\int_0^{2\pi}\frac{[\boldsymbol{\sigma}(t)-\boldsymbol{\gamma}(\tau)]\cdot\boldsymbol{\xi}(t)}{\|\boldsymbol{\sigma}(t)-\boldsymbol{\gamma}(\tau)\|^2}\|\boldsymbol{\gamma}'(\tau)\|\,u(\tau)\,\mathrm{d}\tau.$$

Step 4: Rewriting the partial derivatives of the parametrized single layer operators. In accordance with Kress [20, pp. 513], we introduce the following parametrized double layer operators: For all $t \in [0, 2\pi)$ and $A \in \{\Sigma, \Gamma\}$, define the (parametrized) double layer operators

$$K_{A\Sigma}\, u(t) = \frac{1}{2\pi} \int_0^{2\pi} \frac{[z_A(\tau) - \boldsymbol{\sigma}(t)] \cdot \boldsymbol{\sigma}'(\tau)^\perp}{\|z_A(\tau) - \boldsymbol{\sigma}(t)\|^2}\, u(\tau)\, \mathrm{d}\tau$$

and the operators

$$L_{\Sigma A}\, u(t) = \frac{1}{2\pi} \int_0^{2\pi} \frac{[\boldsymbol{\sigma}(t) - z_A(\tau)] \cdot \mathbf{e}_r(t)}{\|\boldsymbol{\sigma}(t) - z_A(\tau)\|^2} \|z_A'(\tau)\|\, u(\tau)\, \mathrm{d}\tau.$$

By [20, Eqs. (3.8)–(3.10)], we have

$$\begin{aligned}
D_{\boldsymbol{\sigma}} S_{\Sigma\Sigma}[\boldsymbol{\gamma}_0, \boldsymbol{\sigma}_0].\boldsymbol{\xi}\, u &= K_{\Sigma\Sigma}\, (\alpha_0 \xi u) + \xi\, L_{\Sigma\Sigma} u + S_{\Sigma\Sigma}(\alpha_0 \kappa_0 \xi u), \\
D_{\boldsymbol{\sigma}} S_{\Sigma\Gamma}[\boldsymbol{\gamma}_0, \boldsymbol{\sigma}_0].\boldsymbol{\xi}\, u &= \xi\, L_{\Sigma\Gamma} u, \\
D_{\boldsymbol{\sigma}} S_{\Gamma\Sigma}[\boldsymbol{\gamma}_0, \boldsymbol{\sigma}_0].\boldsymbol{\xi}\, u &= K_{\Gamma\Sigma}(\alpha_0 \xi u) + S_{\Gamma\Sigma}(\alpha_0 \kappa_0 \xi u),
\end{aligned}$$

where κ_0 is the curvature of Σ_0 and α_0 is

$$\alpha_0 = \frac{r_{\Sigma,0}}{\sqrt{r_{\Sigma,0}^2 + (r_{\Sigma,0}')^2}}.$$

Step 5: Checking the injectivity of the partial derivative. We now claim that the linear operator $D_{\boldsymbol{\sigma},g} F(\boldsymbol{\gamma}_0, \boldsymbol{\sigma}_0, g_0)$, defined on $\mathcal{C}^k(\mathbb{S}^1) \times \mathrm{H}^{-1/2}(\mathbb{S}^1)$ into $\mathrm{H}^{1/2}(\mathbb{S}^1) \times \mathrm{H}^{-1/2}(\mathbb{S}^1)$, is injective. Assume that $\boldsymbol{\xi} \in \mathcal{C}^k(\mathbb{S}^1)$ and $h \in \mathrm{H}^{-1/2}(\mathbb{S}^1)$ satisfy the linear system

$$\begin{aligned}
-D_{\boldsymbol{\sigma}} S_{\Gamma\Sigma}[\boldsymbol{\gamma}_0, \boldsymbol{\sigma}_0].\boldsymbol{\xi}\, g_0 + S_{\Gamma\Sigma}[\boldsymbol{\gamma}_0, \boldsymbol{\sigma}_0]\, h = 0, \\
-\lambda\, D_{\boldsymbol{\sigma}} S_{\Sigma\Gamma}[\boldsymbol{\gamma}_0, \boldsymbol{\sigma}_0].\boldsymbol{\xi}\, 1 + D_{\boldsymbol{\sigma}} S_{\Sigma\Sigma}[\boldsymbol{\sigma}_0].\boldsymbol{\xi}\, g_0 + S_{\Sigma\Sigma}[\boldsymbol{\gamma}_0, \boldsymbol{\sigma}_0]\, h = 0.
\end{aligned} \tag{2.8}$$

Using the jump relations of the normal derivative of single layer potential [19, Theorem 7.30], the solution u_0 of (2.1) satisfies for $\mathbf{x}$ on Σ

$$\nabla u_0(\mathbf{x}) = \frac{1}{2\pi} \int_\Sigma \frac{\mathbf{y} - \mathbf{x}}{\|\mathbf{x} - \mathbf{y}\|^2}\, g_0(\mathbf{y})\, \mathrm{d}\varsigma_{\mathbf{y}} - \frac{\lambda}{2\pi} \int_\Gamma \frac{\mathbf{y} - \mathbf{x}}{\|\mathbf{x} - \mathbf{y}\|^2} \mathrm{d}\varsigma_{\mathbf{y}} + \frac{1}{2} g_0(\mathbf{x}) \mathbf{n}(\mathbf{x}).$$

Hence, in view of $\nabla u_0 = g_0 \mathbf{n}$ on Σ_0 and $\mathbf{e}_r \cdot (\mathbf{n} \circ \boldsymbol{\sigma}_0) \equiv \alpha_0$, we arrive at

$$-\lambda\, L_{\Sigma\Gamma}\, 1 + L_{\Sigma\Sigma}\, g_0 = \frac{1}{2} \alpha_0 g_0,$$

so that the linear system (2.8) can be rewritten as

$$\begin{aligned}
-K_{\Gamma\Sigma}[\boldsymbol{\gamma}_0, \boldsymbol{\sigma}_0](\alpha_0 \xi g_0) - S_{\Gamma\Sigma}[\boldsymbol{\gamma}_0, \boldsymbol{\sigma}_0](\alpha_0 \kappa_0 \xi g_0) + S_{\Gamma\Sigma}[\boldsymbol{\gamma}_0, \boldsymbol{\sigma}_0]\, h = 0, \\
\frac{1}{2} g_0 \xi \alpha_0 + K_{\Sigma\Sigma}[\boldsymbol{\gamma}_0, \boldsymbol{\sigma}_0](\alpha_0 \xi g_0) + S_{\Sigma\Sigma}[\boldsymbol{\gamma}_0, \boldsymbol{\sigma}_0](\alpha_0 \kappa_0 \xi g_0) + S_{\Sigma\Sigma}[\boldsymbol{\gamma}_0, \boldsymbol{\sigma}_0]\, h = 0.
\end{aligned} \tag{2.9}$$

We set

$$\varkappa = (\alpha_0 \xi) \circ (\boldsymbol{\gamma}_0)^{-1} \in \mathrm{H}^{1/2}(\Gamma) \text{ and } \vartheta = h \circ \boldsymbol{\sigma}_0^{-1} \in \mathrm{H}^{-1/2}(\Sigma),$$

and define the function v on $\mathbb{R}^2 \setminus \Gamma$ as the potential

$$v(\mathbf{x}) = \int_{\mathbf{\Gamma}} \left(\frac{\partial \mathbf{G}(\mathbf{x},\mathbf{y})}{\partial \boldsymbol{n}_{\mathbf{y}}} + \kappa_{\mathbf{0}} \mathbf{G}(\mathbf{x},\mathbf{y}) \right) \varkappa(\mathbf{y}) \mathrm{d}\varsigma_{\mathbf{y}} + \int_{\mathbf{\Sigma}} \mathbf{G}(\mathbf{x},\mathbf{y}) \vartheta(\mathbf{y}) \mathrm{d}\varsigma_{\mathbf{y}}.$$

We now claim that $v = 0$ in $\mathbb{R}^2$ by separating the plane into K, the domain $D \setminus \overline{K}$ and the complement of D. The conclusion that $\varkappa$ and ϑ are 0 and then that $\boldsymbol{\xi}$ and h are also 0 follows from the jump conditions and the remark that $\mathbf{e}_r \cdot (\mathbf{n} \circ \boldsymbol{\sigma}_0) \equiv \alpha_0 \geq 0$.

Let us prove the claim $v = 0$. Combining the jump relations for such a potential (see [19, Theorem 7.30, Section 7-5]) and the two previous relations from (2.9), we obtain that:

- It holds $v = 0$ on Σ and, by uniqueness of the solution of interior Dirichlet problem, we infer $v = 0$ in K.
- In a second step, we deduce that the limit v_+, obtained by approaching Γ form outside D, satisfies $v_+ = 0$ on Γ. We thus deduce that $v = 0$ in $\mathbb{R}^2 \setminus \overline{D}$.
- In a third and last step, we conclude that the limit v_-, obtained by approaching Γ from the interior of D, satisfies the Fourier-Robin condition

  $$\partial_{\boldsymbol{n}} v_- + \kappa_0 v_- = 0 \text{ on } \Gamma.$$

  Hence, the restriction of v to the domain $D \setminus \overline{K}$ is the solution of the boundary value problem

  $$\begin{aligned} \Delta v &= 0 \text{ in } D \setminus \overline{K}, \\ v &= 0 \text{ on } \Gamma, \\ \partial_{\boldsymbol{n}} v + \kappa_0 v &= 0 \text{ on } \Sigma. \end{aligned}$$

  Therefore, integration by parts leads to

  $$0 \leq \int_{D \setminus \overline{K}} |\nabla v|^2 = - \int_{\Gamma} \kappa |v|^2 \leq 0,$$

  where the last inequality comes from the convexity of K that infers the convexity of D by the Henrot-Shahgholian Theorem and then that $\kappa \geq 0$. Hence, $v = 0$ in $D \setminus \overline{K}$.

Step 6: Conclusion. The claim now follows by applying the implicit function theorem.

3 Random convex sets

In this section, we gather known results from various contexts about random convex compact sets in order to define the confidence region for the Aumann expectation. This will be needed for the numerical simulations.

3.1 Convex sets and support functions

We recall in this section the well-known properties of convex sets that we shall use. The reader interested in the proofs of these properties is refered to the reference monograph of Schneider [23].

We denote by $\mathfrak{C}^d$ the set of non-empty compact subsets of $\mathbb{R}^d$. Endowed with the Hausdorff distance $d_{\mathfrak{H}}$, defined by

$$d_{\mathfrak{H}}(K_1, K_2) = \sup\big\{\{d(x, K_1),\ x \in K_2\} \cup \{d(x, K_2),\ x \in K_1\}\big\},$$

it is a complete metric space (see Theorem 1-8-3 in [23]). In $(\mathfrak{C}^d, d_{\mathfrak{H}})$, every closed bounded set is compact (Theorem 1-8-4 in [23]). Each bounded sequence in $(\mathfrak{C}^d, d_{\mathfrak{H}})$ has a converging subsequence (Theorem 1-8-5 in [23]). The set of compact convex subsets $\mathfrak{K}^d$ of $\mathbb{R}^d$ is a closed subset of $\mathfrak{C}^d$. In particular, the selection theorem of Blaschke states that every bounded sequence in $\mathfrak{K}^d$ admits a converging subsequence that converges to a compact convex set.

On the support function of a convex set. A key ingredient for the definition of the Aumann expectation of a random convex set is the support function. Let us recall its definition and its main properties. Convex sets are parametrized by their support function h_K defined on $\mathbb{R}^d$ by

$$h_K(x) = \sup\{x \cdot y,\ y \in K\}.$$

The support function of a convex set is homogeneous of degree one and hence can be restricted to the unit sphere without loss of generality. Let $\widetilde{h}_K$ be the restriction of h_K to the unit sphere. Let us introduce the parametrization mapping $\boldsymbol{\Upsilon}$ defined by

$$\begin{aligned} \boldsymbol{\Upsilon}:\ \mathfrak{K}^d &\to \mathcal{C}^0(\mathbb{S}^{d-1}) \\ K &\mapsto \widetilde{h}_K. \end{aligned}$$

A crucial property is the isometric connection between the Hausdorff distance and the L^∞-norm on $\mathcal{C}^0(\mathbb{S}^{d-1})$: for all $K_1,\ K_2 \in \mathfrak{K}^d$,

$$d_{\mathfrak{H}}(K_1, K_2) = \|\widetilde{h}_{K_1} - \widetilde{h}_{K_2}\|_{\mathrm{L}^\infty(\mathbb{S}^{d-1})}. \tag{3.1}$$

From support functions to convex sets. In order to use the support function in numerical computations, we need a way to reconstruct a convex set from a support function. This is the role of the envelope operator which is defined as

$$\begin{aligned} \mathcal{E} : \mathcal{C}^1(\mathbb{S}^{d-1}, \mathbb{R}) &\to \mathcal{C}^1(\mathbb{S}^{d-1}, \mathbb{R}^d) \\ \widetilde{h} &\mapsto \mathcal{E}\big[\widetilde{h}\big], \end{aligned}$$

where, for all $\overline{x} \in \mathbb{S}^{d-1}$, one sets

$$\mathcal{E}[\widetilde{h}](\overline{x}) = h(\overline{x})\overline{x} + \nabla_\tau \widetilde{h}(\overline{x}).$$

This operator allows to reconstruct a convex set whose restricted support is $\widetilde{h}$. Notice that this point has been investigated in a recent work of Antunes and Bogosel [3].

Example 3.1 In the planar case, one gets simply $\widetilde{h} : [0, 2\pi) \to \mathbb{R}$ and a parametrization of a set whose support function is $\widetilde{h}$ is

$$\mathcal{E}(\widetilde{h}) : \theta \mapsto \widetilde{h}(\theta)\mathbf{e}_r(\theta) + \widetilde{h}'(\theta)\mathbf{e}_r'(\theta).$$

In the three-dimensional case, the unit sphere is endowed with the usual spherical coordinates so that $\widetilde{h}:\ [0,2\pi)\times[0,\pi]\to\mathbb{R}$. We thus get

$$\mathcal{E}(\widetilde{h}):(\theta,\varphi)\mapsto\widetilde{h}(\theta,\varphi)\mathbf{e}_r(\theta)+\partial_\theta\widetilde{h}(\theta)\mathbf{e}_\theta(\theta,\varphi)+\frac{1}{\sin(\theta)}\partial_\varphi\widetilde{h}(\theta)\mathbf{e}_\theta(\theta,\varphi).$$

Let us recall that the Frenet vectors satisfy the relations

$$\begin{array}{lllllllll}\partial_\theta\mathbf{e}_r&=&\mathbf{e}_\theta&\partial_\theta\mathbf{e}_\theta&=&-\mathbf{e}_r&\partial_\theta\mathbf{e}_\varphi&=&-\sin\theta\ \mathbf{e}_r\\ \partial_\varphi\mathbf{e}_r&=&\sin\theta\ \mathbf{e}_\varphi&\partial_\varphi\mathbf{e}_\theta&=&\cos\theta\ \mathbf{e}_\varphi&\partial_\varphi\mathbf{e}_\varphi&=&-\cos\theta\ \mathbf{e}_\theta\end{array}$$

Among continuous functions of the unit sphere, some are support functions on a convex set and some are not – support functions are sublinear functions. Recall that a function is sublinear if it satisfies both:

$$\forall(x,y)\in\mathbb{R}^d,\ \lambda\geq 0:\ f(\lambda x)=\lambda f(x)\text{ and }f(x+y)\leq f(x)+f(y).$$

Vice versa, each sublinear function is the support function of a convex set (Theorem 1-7-1 [23]). As a consequence, $\boldsymbol{\Upsilon}(\mathfrak{K}^d)$ is a convex cone of the vector space $\mathcal{C}^0(\mathbb{S}^{d-1})$. It is a closed subset. More precisely, if a sequence of support functions converges pointwise, then it converges uniformly to a support function (Theorem 1-8-15 [23]). Let us notice that the vector space generated by $\boldsymbol{\Upsilon}(\mathfrak{K}^d)$ is dense in $\mathcal{C}^0(\mathbb{S}^{d-1})$.

There is no clear local characterization of sublinear functions. However, when using this parametrization on convex sets in a computation, one needs a practical way to characterize the fact that the envelope operator maps the function to a convex set. One way is to use the curvature. For a convex set, the curvatures is positive everywhere. This remark provides a characterization of support functions of regular convex sets by the set of continuous functions on the unit sphere in terms of differential inequalities that should be satisfied pointwise.

3.2 Random sets

For general definitions and properties of random sets, we refer to the book of Molchanov [21] and, for the specific case of random compact convex sets, to the article [22] of Puri and Ralescu. Notice that, as $\mathfrak{C}^d$ is not a vector space, the concept of expectation is not so easy to establish and various definitions exist. We chose in this work to use the notion of Aumann expectation.

Let us start by recalling the definition a of random convex sets. Let $(\Omega,\mathcal{F},\mathbb{P})$ be a complete probability space.

Definition 3.2 *A random compact set in $\mathbb{R}^d$ is a Borel measurable function $X:\Omega\to\mathfrak{C}^d$. A random compact set X is a random convex compact set in $\mathbb{R}^d$ if its realizations are almost surely convex.*

Remark 3.3 X is a random convex compact set in $\mathbb{R}^d$ if and only if the support function $\widetilde{h}_X(u)$ is a random variable for every $u\in\mathbb{S}^{d-1}$. Owing to that property, one deduces that the distribution of a convex compact set is characterized by the values of the function $C_X(K)=\mathbb{P}(X\subset K)$ for $K\in\mathfrak{K}^d$.

We are in position to define the Aumann expectation of a random convex compact set.

Definition 3.4 *Let X be a random compact convex set. The Aumann integral of X is defined as*

$$\mathbb{E}_A(X)=\{\mathbb{E}(\xi)\mid\xi\in\mathrm{L}^1(\Omega,\mathcal{F},\mathbb{P}),\ \xi(\omega)\in X(\omega)\ a.s.\},\tag{3.2}$$

where $\mathbb{E}(\xi)$ denotes the classical expectation.

Remark 3.5 1. Here $\xi : \Omega \to \mathbb{R}^d$ is called a "selection" of X.

2. If the distribution of X is non-atomic and if $\mathbb{E}\big(d_{\mathfrak{H}}(X, \{0\})\big) < \infty$, then $\mathbb{E}_A(X)$ is compact convex and it is, owing to the Hörmander embedding, the unique convex compact set which satisfies

$$\mathbb{E}\big(\widetilde{h}_X(u)\big) = \widetilde{h}_{\mathbb{E}_A(X)}(u)$$

for all $u \in \mathbb{S}^{d-1}$.

This notion of expectation has been studied much. In particular, one has the following deep limit theorems we quote from the works of Puri and Weil.

Theorem 3.6 (Strong law of large numbers (Puri and Ralescu [22])) *Let $(X_n)_n$ be i.i.d. random compact convex sets in $\mathbb{R}^d$ such that $\mathbb{E}(d_{\mathfrak{H}}(X_1, \{0\})) < \infty$. Then*

$$\frac{X_1 + \cdots + X_n}{n} \xrightarrow[n\to\infty]{} \mathbb{E}_A(X_1) \ a.s., \tag{3.3}$$

where the convergence holds in the Hausdorff metric sense.

Theorem 3.7 (Central limit theorem (Weil [26])) *Let $(X_n)_n$ be i.i.d. random compact convex sets in $\mathbb{R}^d$ such that $\mathbb{E}\big(d_{\mathfrak{H}}(X_1, \{0\})^2\big) < \infty$. We denote*

$$\overline{X}_n = \frac{X_1 + \cdots + X_n}{n}.$$

Then

$$\sqrt{n}\left(\widetilde{h}_{\overline{X}_n} - \widetilde{h}_{\mathbb{E}_A(X_1)}\right) \xrightarrow[n\to\infty]{\mathcal{D}} Z, \tag{3.4}$$

where Z is a centered Gaussian $\mathcal{C}(\mathbb{S}^{d-1})$-valued random variable, and as corollary

$$\sqrt{n} d_{\mathfrak{H}}\left(\overline{X}_n, \mathbb{E}_A(X_1)\right) \xrightarrow[n\to\infty]{\mathcal{D}} \|Z\|_\infty. \tag{3.5}$$

With the aforementioned central limit theorem at hand, a confidence region for the Aumann expectation can be defined. This was introduced in the work of Choirat and al. [8].

Let ϵ be a nonnegative real number. We first define the inflated and deflated copies of the empirical estimator $\overline{X}_n$: set $K_n^+(\epsilon)$ and $K_n^-(\epsilon)$ be the two compact convex sets defined by

$$K_n^+(\epsilon) = \left\{x \in \mathbb{R}^d,\ d(x, \overline{X}_n) \le \epsilon\right\}$$

and

$$K_n^-(\epsilon) = \left\{x \in \overline{X}_n,\ d(x, \mathbb{R}^d \setminus \overline{X}_n) \le \epsilon\right\}.$$

If B denotes the unit ball, these definitions can also be written as

$$K_n^+(\epsilon) = \overline{X}_n + \epsilon B \text{ and } K_n^-(\epsilon) + \epsilon B = \overline{X}_n.$$

Using the property describing the Minkowski sum by the support function of convex sets, we obtain the relations

$$\widetilde{h}_{K_n^\pm} = \widetilde{h}_{\overline{X}_n} \pm \epsilon.$$

Given a real number $\alpha \in [0,1]$, one seeks to determine ϵ such that

$$\mathbb{P}\left(K_n^-(\epsilon) \subset \mathbb{E}_A(X_1) \subset K_n^+(\epsilon)\right) \geq 1-\alpha.$$

In terms of support functions, we can write

$$\begin{aligned} \mathbb{P}\big(K_n^-(\epsilon) \subset \mathbb{E}_A(X_1) \subset K_n^+(\epsilon)\big) &= \mathbb{P}\big(\widetilde{h}_{\overline{X}_n} - \epsilon \leq \widetilde{h}_{\mathbb{E}_A(X_1)} \leq \widetilde{h}_{\overline{X}_n} + \epsilon\big) \\ &= \mathbb{P}\big(\big\|\widetilde{h}_{\mathbb{E}_A(X_1)} - \widetilde{h}_{\overline{X}_n}\big\|_\infty \leq \epsilon\big) \end{aligned} \tag{3.6}$$

by using the calculation rules for support functions restricted to the unit sphere. Notice that we have reduced, thanks to Weil's limit theorem, the problem of the confidence region to the estimation of a quantile for a real valued random variable. In practice, we can invoke the central limit theorem 3.4 in order to see that $\widetilde{h}_{\mathbb{E}_A(X_1)} - \widetilde{h}_{\overline{X}_n}$ follows approximately a centered normal distribution. In that context, one needs to know the distribution of the limit law $\|Z\|_\infty$. Indeed, under this knowledge, we obtain the following asymptotic confidence region for the expectation of the random free boundary.

Definition 3.8 *If one knows a real number C such that $\mathbb{P}(\|Z\|_\infty \leq C) \geq 1-\alpha$, then one has*

$$\lim_{n\to+\infty} \mathbb{P}\left(K_n^-\left(\frac{C}{\sqrt{n}}\right) \subset \mathbb{E}_A(X_1) \subset K_n^+\left(\frac{C}{\sqrt{n}}\right)\right) \geq 1-\alpha.$$

Not much can be said about the distribution $\|Z\|_\infty$ from the theoretical point of view. Hence, one can only approximate it by sampling. With respect to the heavy computational cost, we follow a bootstrap method as suggested in [8]. This approach will be proposed in the Section 4.5.

4 Computing free boundaries

We now present the numerical method we propose to perform the computations. In order to compute the expectation of the domain $D(\omega)$, we have to be able to determine the free boundary $\Gamma(\omega)$ for each specific realization $\omega \in \Omega$ of the interior boundary $\Sigma(\omega)$. For sake of simplicity in representation, we omit the random parameter $\omega \in \Omega$ in this section, i.e., we assume that $\omega \in \Omega$ is fixed.

4.1 Trial method

In the following, we identify the sought free boundary Γ with the radial function $r \in \mathcal{C}^2_{\text{per}}([0,2\pi])$ which parametrizes the boundary in accordance with

$$\boldsymbol{\gamma} : [0,2\pi] \to \Gamma, \quad \boldsymbol{\gamma}(\varphi) = r(\varphi)\begin{bmatrix}\cos\varphi \\ \sin\varphi\end{bmatrix}.$$

Then, we employ the so-called trial method, which is a fixed point type iterative method, to determine the unknown function r.

Suppose that the current boundary in the k-th iteration is Γ_k and let the current state u_k satisfy

$$\begin{aligned} \Delta u_k &= 0 \qquad \text{in } D_k, \\ u_k &= 1 \qquad \text{on } \Sigma, \\ -\frac{\partial u_k}{\partial \mathbf{n}} &= \lambda \qquad \text{on } \Gamma_k. \end{aligned} \tag{4.1}$$

In order to find an improved boundary Γ_{k+1} being a "better" approximation to the free boundary problem (2.1), we modify the old boundary Γ_k with respect to the radial direction. This is achieved by the update rule

$$\boldsymbol{\gamma}_{k+1} = \boldsymbol{\gamma}_k + \delta r_k \mathbf{e}_r.$$

The increment function $\delta r_k \in \mathcal{C}^2_{\mathrm{per}}([0, 2\pi])$ is chosen such that the desired homogeneous Dirichlet boundary condition is approximately satisfied at the updated boundary Γ_{k+1}, i.e.,

$$0 = u_k \circ \boldsymbol{\gamma}_{k+1} \approx u_k \circ \boldsymbol{\gamma}_k + \left(\frac{\partial u_k}{\partial \mathbf{e}_r} \circ \boldsymbol{\gamma}_k \right) \delta r_k \quad \text{on } [0, 2\pi], \tag{4.2}$$

where u_k is supposed to be smoothly extended into the exterior of the domain D_k. For numerical reasons, we decompose the derivative of u_k in the direction $\mathbf{e}_r$ into its normal and tangential components

$$\frac{\partial u_k}{\partial \mathbf{e}_r} = \frac{\partial u_k}{\partial \mathbf{n}} \langle \mathbf{e}_r, \mathbf{n} \rangle + \frac{\partial u_k}{\partial \mathbf{t}} \langle \mathbf{e}_r, \mathbf{t} \rangle \quad \text{on } \Gamma_k \tag{4.3}$$

to arrive finally at the following iterative scheme, which is known to be linearly convergent, cf. [13, 14, 25]:

(1) Choose an initial guess Γ_0 of the free boundary.

(2a) Solve the boundary value problem with the Neumann boundary condition on the free boundary Γ_k.

(2b) Update the free boundary Γ_k such that the Dirichlet boundary condition is approximately satisfied at the new boundary Γ_{k+1}:

$$\delta r_k = -\frac{u_k}{\frac{\partial u_k}{\partial \mathbf{e}_r}} = -\frac{u_k}{\lambda \langle \mathbf{n}, \mathbf{e}_r \rangle + \frac{\partial u_k}{\partial \mathbf{t}} \langle \mathbf{t}, \mathbf{e}_r \rangle} \tag{4.4}$$

(3) Repeat step (2) until the process becomes stationary up to a specified accuracy.

Notice that the update equation (4.4) is always solvable at least in a neighbourhood of the optimum free boundary Γ since there it holds $-\partial u / \partial \mathbf{e}_r = f \langle \mathbf{e}_r, \mathbf{n} \rangle > 0$ due to $\partial u_k / \partial \mathbf{t} = 0$, $f > 0$ and $\langle \mathbf{e}_r, \mathbf{n} \rangle > 0$ for starlike domains.

4.2 Discretizing the free boundary

For the numerical computations, we discretize the radial function r_k associated with the boundary Γ_k by a trigonometric polynomial according to

$$r_k(\varphi) = \frac{a_0}{2} + \sum_{\ell=1}^{p-1} \big\{ a_\ell \cos(\ell\varphi) + b_\ell \sin(\ell\varphi) \big\} + \frac{a_p}{2} \cos(p\varphi). \tag{4.5}$$

This obviously ensures that r_k is always an element of $\mathcal{C}^2_{\mathrm{per}}([0, 2\pi])$. To determine the increment function δr_k, represented likewise by a trigonometric polynomial, we insert the $m \geq 2p$ equidistantly distributed points $\varphi_i = 2\pi i / m$ into the update equation (4.4):

$$\delta r_k = -\frac{u_k}{\lambda \langle \mathbf{n}, \mathbf{e}_r \rangle + \frac{\partial u_k}{\partial \mathbf{t}} \langle \mathbf{t}, \mathbf{e}_r \rangle} \quad \text{in all the points } \varphi_1, \ldots, \varphi_m.$$

This is a discrete least-squares problem which can simply be solved by the normal equations. In view of the orthogonality of the Fourier basis, this means just a truncation of the respective trigonometric polynomial.

4.3 Computing the support function

Having the final boundary Γ at hand, we can compute its support function. The definition of the support function

$$p(\varphi) = \sup_{\mathbf{x}\in D_k} \langle \mathbf{x}, \mathbf{e}_r(\varphi)\rangle, \quad \varphi \in [0, 2\pi),$$

amounts to the computation of

$$p(\varphi) = \max_{\psi\in[0,2\pi)} \langle \boldsymbol{\gamma}(\psi), \mathbf{e}_r(\varphi)\rangle = \max_{\psi\in[0,2\pi)} r(\psi)\langle \mathbf{e}_r(\psi), \mathbf{e}_r(\varphi)\rangle, \quad \varphi \in [0, 2\pi).$$

This computation is performed for n discrete angles $\varphi_i = 2\pi i/n$, $i = 0, 1, \ldots, n-1$, and $\psi_j = 2\pi j/n$, $j = 0, 1, \ldots, n-1$. Finally, a Fourier series representing the periodic function $p(\varphi)$ is computed.

4.4 Boundary integral equations

Our approach to determine the solution u_k of the state equation (4.1) relies on the reformulation as a boundary integral equation.

The equation (2.4) in combination with (2.5) and (2.6) indicates the Neumann-to-Dirichlet map, which for problem (4.1) induces the following system of integral equations:

$$\begin{bmatrix} -(\frac{1}{2}I + \mathcal{K}_{\Gamma\Gamma}) & \mathcal{V}_{\Sigma\Gamma} \\ -\mathcal{K}_{\Gamma\Sigma} & \mathcal{V}_{\Sigma\Sigma} \end{bmatrix} \begin{bmatrix} u_k|_\Gamma \\ \frac{\partial u_k}{\partial \mathbf{n}}\big|_\Sigma \end{bmatrix} = \begin{bmatrix} \mathcal{V}_{\Gamma\Gamma} & \mathcal{K}_{\Sigma\Gamma} \\ \mathcal{V}_{\Gamma\Sigma} & \left(\frac{1}{2}I + \mathcal{K}_{\Sigma\Sigma}\right) \end{bmatrix} \begin{bmatrix} \lambda \\ 1 \end{bmatrix}. \tag{4.6}$$

The boundary integral operator on the left hand side of this coupled system of boundary integral equation is continuous and satisfies a Gårding inequality with respect to the product Sobolev space $\mathrm{L}^2(\Gamma) \times \mathrm{H}^{-1/2}(\Sigma)$ provided that $\mathrm{diam}(D) < 1$. Since its injectivity follows from potential theory, this system of integral equations is uniquely solvable according to the Riesz-Schauder theory.

The next step to the solution of the boundary value problem is the numerical approximation of the integral operators included in (4.6) which first requires the parameterization of the integral equations. To that end, we insert the parameterizations $\boldsymbol{\sigma}$ and $\boldsymbol{\gamma}_k$ of the boundaries Σ and Γ_k, respectively. For the approximation of the unknown Cauchy data, we use the collocation method based on trigonometric polynomials. Applying the trapezoidal rule for the numerical quadrature and the regularization technique along the lines of [19] to deal with the singular integrals, we arrive at an exponentially convergent Nyström method provided that the data and the boundaries and thus the solution are arbitrarily smooth.

4.5 Bootstrapping for the confidence interval

The main difficulty one has to face here is the heavy computational cost of the confidence region as it requires to compute the distribution of the limit law $\|Z\|_\infty$. The first idea is then of course to approximate it by a finite sampling approximation $\sqrt{n}\big\|\widetilde{h}_{\mathbb{E}_A(X_1)} - \widetilde{h}_{\overline{X}_n}\big\|_\infty$. However, this is almost untractable since it requires to solve too much free boundary problems. Following the references [8, 18], we propose to use a bootstrapping method in order to reduce the number of needed solutions to the free boundary problem.

The procedure we propose in order to evaluate a confidence interval is the following:

From $k = 1$ to N (Monte-Carlo method) do

1. Take p directions on the sphere $\mathbb{S}^{d-1}$ and simulate n discretized support functions $\mathbf{h}_{X_1}, \dots, \mathbf{h}_{X_n}$. Note that each discretized support function is a vector in $\mathbb{R}^p$.

2. Obtain then the empirical distribution associated and simulate for $b = 1, \dots, J$ samples $\mathbf{h}_1^b, \dots, \mathbf{h}_n^b$ following this distribution. This is the bootstrap step which gives

$$\mathbf{h}_n^* = \frac{1}{J}\left(\sum_{b=1}^{J}\left[\frac{1}{n}\sum_{i=1}^{n}\mathbf{h}_i^b\right]\right).$$

3. The quantity $\mathbf{h}_n^* - \mathbf{h}_{\overline{X}_n}$ approximates of $\mathbf{h}_{\mathbb{E}_A(X_1)} - \mathbf{h}_{\overline{X}_n}$, thus calculate $\left\|\mathbf{h}_n^* - \mathbf{h}_{\overline{X}_n}\right\|_\infty$. Note that it holds the identity

$$\mathbf{h}_{\overline{X}_n} = \overline{\mathbf{h}_{X_n}}.$$

After these computations, we have N values of $\left\|\mathbf{h}_n^* - \mathbf{h}_{\overline{X}_n}\right\|_\infty$. Denote by $\hat{F}_N$ the empirical cumulative distribution associated with $\left\|\mathbf{h}_n^* - \mathbf{h}_{\overline{X}_n}\right\|_\infty$, given by

$$\hat{F}_N(x) = \frac{1}{N}\#\left\{\left\|\mathbf{h}_n^* - \mathbf{h}_{\overline{X}_n}\right\|_\infty \leq x\right\}. \tag{4.7}$$

Finally, we determine $\epsilon > 0$ such that $\hat{F}_N(\epsilon) \geq 1 - \alpha$. The quantify ϵ defines the size of the desired confidence interval to the confidence level α.

5 Numerical results

5.1 First experiment: smooth support function

In our first experiment, we consider a random support function $p(\varphi)$ which is computed by a random Fourier series. Namely, we define

$$p(\varphi) = 0.1\left(1 + \frac{a_0(\omega)}{2} + \sum_{\ell=1}^{\infty}\frac{1}{\ell^4}\left\{a_\ell(\varphi)\cos(\ell\varphi) + b_\ell(\varphi)\sin(\ell\varphi)\right\}\right), \tag{5.1}$$

where $a_\ell(\varphi)$ and $b_\ell(\varphi)$ are independent and uniformly distributed random variables in $[-1/2, 1/2]$. The cubic decay of the Fourier coefficients ensures that $p \in \mathcal{C}^3_{\text{per}}([0, 2\pi])$ and, hence, the realization of $\Sigma(\omega)$ is always a $\mathcal{C}^2$-smooth boundary. In practice, we truncate the infinite Fourier series of the support function after $\ell = 50$ terms.

The specific setup for our the numerical solution of the free boundary problem is as follows. We consider the desired Dirichlet data to be $\lambda = 10$. For the numerical solver, 400 equidistant collocation points per boundary are used in the boundary element method and also for the calculation of the update and the support function in accordance with Subsections 4.2 and 4.3. The initial guess of the trial method is a ball with radius $r_0 = 0.2$. We stop the trial method if the L^∞-norm of the Dirichlet data at the free boundary are smaller than 10^{-6}. In all, we compute $M = 10\,000$ samples of the free boundary problem. Some of these random samples are found in Figure 1, where the gray matter is the final domain $D(\omega_i)$ while the coloured lines indicate the iterates of the trial method.

The computed mean boundaries are found in Figure 2. The interior mean boundary is a circle of radius 0.1 while the exterior mean boundary is circle of radius 0.176. We mention that, by definition

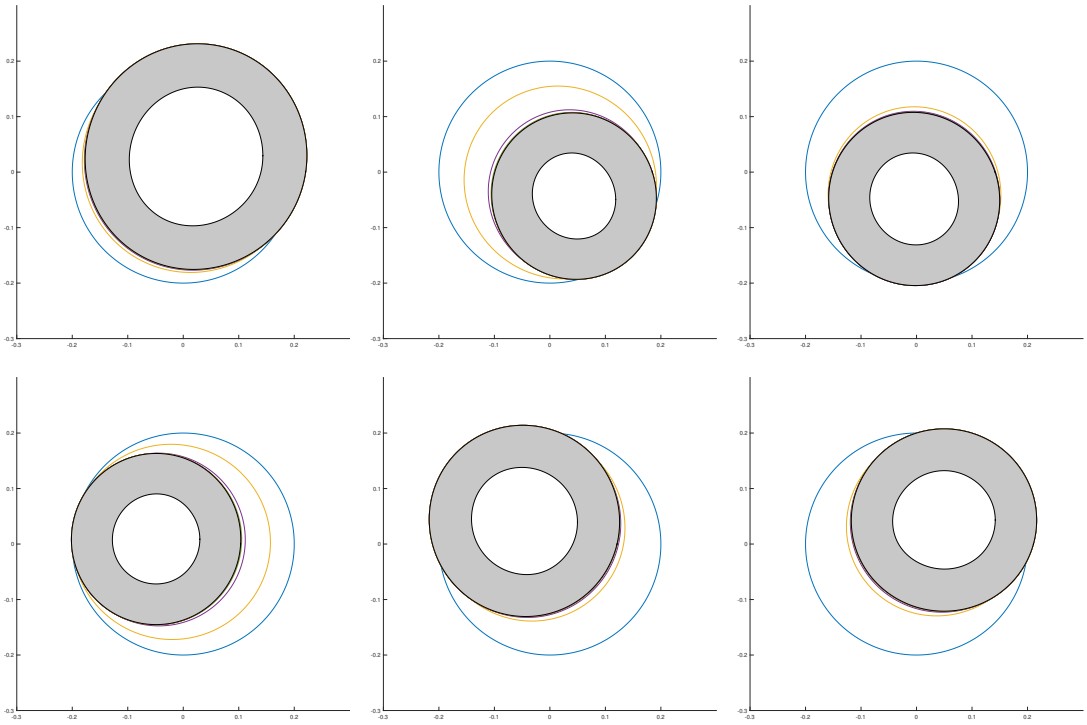

Figure 1: Different realizations of the free boundary problem in case of a smooth random support function as interior boundary.

of the function $p(\varphi)$ in (5.1), in view of $\mathbb{E}(p) \equiv 0.1$ and $\mathbb{E}(p') = 0$, the mean of the support function of the interior boundary is also $\equiv 0.1$, and hence the interior mean boundary is indeed be the circle of radius 0.1. Moreover, by symmetry arguments, the exterior mean boundary should also be a circle, but of unknown radius.

We shall next comment on the computation of the confidence interval. We need to compute the empirical cumulative distribution $\hat{F}_N$ of the random variable $\left\|\mathbf{h}_n^* - \widetilde{\mathbf{h}}_{\overline{X}_n}\right\|_\infty$, compare (4.7). To this end, we distribute the $M = 10\,000$ free boundary computations in accordance with $N = n = 100$ and set $J = 100$ for the bootstrapping. These parameters were chosen so that the total duration of the computations is of the order of two hours on a standard notebook – in our case a MacBook. This results in the empirical cumulative distribution found in Figure 3. The size of the confidence interval is $6.81 \cdot 10^{-3}$ in case of the confidence level $\alpha = 10\,\%$ and $8.37 \cdot 10^{-3}$ in case of the confidence level $\alpha = 5\,\%$. In view of this small confidence interval, the computed circular mean boundaries are quite optimal with high probability.

5.2 Second experiment: polygonal inclusion

In the second experiment, we shall consider convex random polygons with five vertices as interior boundary $\Sigma(\omega)$, which we construct as follows. We draw a uniformly distributed random vector $\boldsymbol{\psi} \in [0, 2\pi]^5$, representing the angles of the vertices, and a random radius $r \in [a, b]$, representing the perimeter where the vertices lie on. Hence, the polygon has the five vertices

$$\mathbf{v}_1 = r\mathbf{e}_r(\psi_1), \quad \mathbf{v}_2 = r\mathbf{e}_r(\psi_2), \quad \dots \quad \mathbf{v}_5 = r\mathbf{e}_r(\psi_5),$$

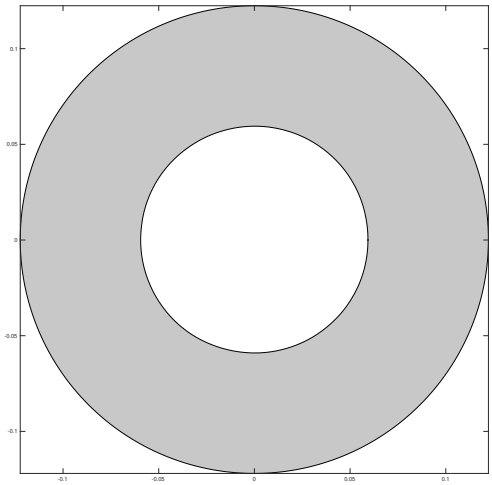

Figure 2: The mean of the support functions of the interior boundary and the exterior boundary in case of the first example.

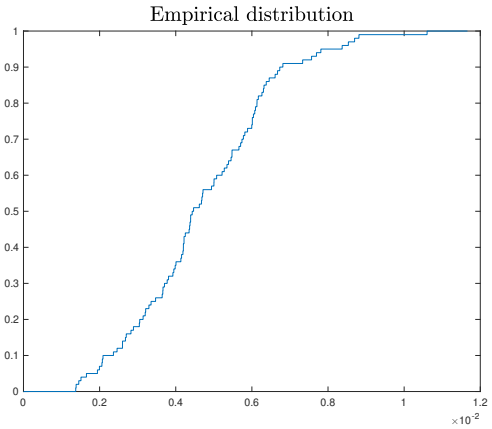

Figure 3: The empirical cumulative distribution $\hat{F}_N$ scaled by the factor $\sqrt{n}$ in case of the first example.

where we assume that $\psi_1 < \psi_2 < \cdots < \psi_5$. In order to avoid degenerate polygons, we further impose the condition that the distance between two subsequent vertices is larger or equal to a prescribed lower bound d. Finally, the barycenter

$$\mathbf{s} = \frac{1}{5} \sum_{i=1}^{5} \mathbf{v}_i$$

of the convex polygon is shifted into $\mathbf{0}$ by the coordinate transform

$$\mathbf{v}_i \mapsto \widehat{\mathbf{v}}_i := \mathbf{v}_i - \mathbf{s}, \quad i = 1, 2, \ldots, 5.$$

In our experiment, we choose the polygon's perimeter bounds as $a = 0.05$, $b = 0.10$, and $d = 0.25$.

We draw again 10 000 samples, where all parameters in the trial method are set as in the first experiment. Some samples are illustrated in Figure 4, where again the gray matter indicates the final domain, which are accompanied by the iterates of the nonlinear solver for the exterior boundary, indicated by lines.

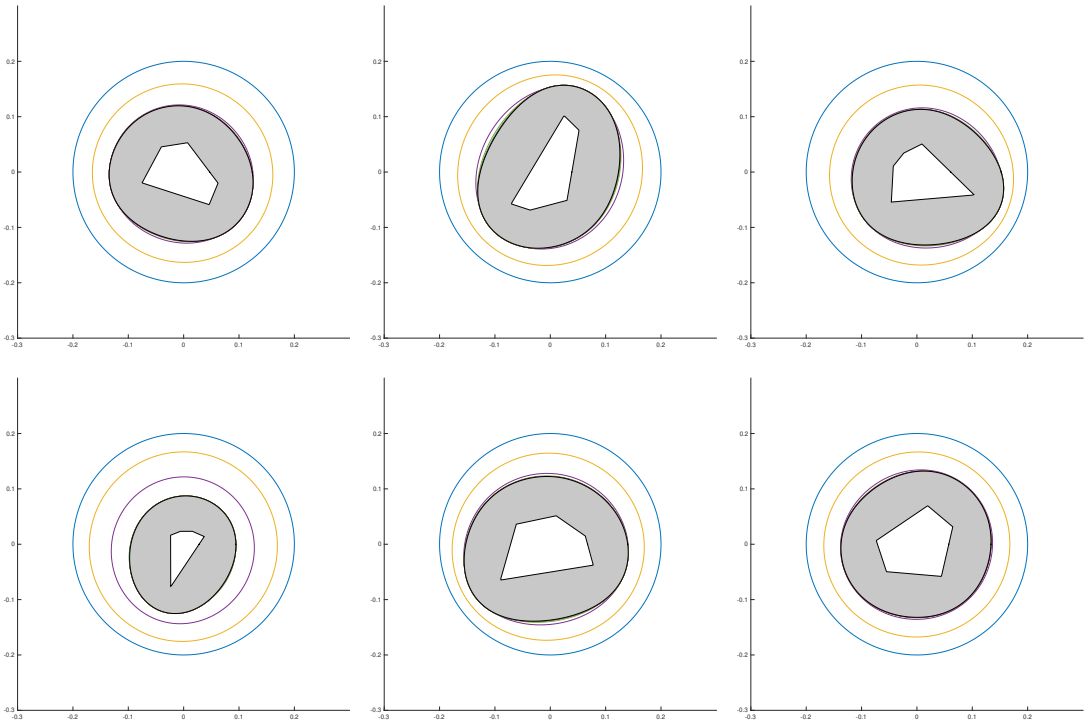

Figure 4: Different realizations of the free boundary problem in case of a convex random polygon as interior boundary.

The computed mean boundaries, which turned out to be (approximately) circles of radius $r_\Sigma = 0.0523$ and $r_\Gamma = 0.128$, are found in Figure 5. Likewise to the first example, it is clear from a symmetry point of view that circular shapes of the mean are expected.

The empirical cumulative distribution $\hat{F}_N$ of the random variable $\left\|\mathbf{h}_n^* - \widetilde{\mathbf{h}}_{\overline{X}_n}\right\|_\infty$ is found in Figure 6. The confidence interval has the size $4.68 \cdot 10^{-4}$ for the confidence level $\alpha = 10\,\%$ and $5.34 \cdot 10^{-4}$ for $\alpha = 5\,\%$. In Figure 7, we plot a zoom of the asymptotic confidence regions for various values of the sample size n in order to illustrate the Definition 3.8. Of course, the sampling size remains small to reach the asymptotic regime.

References

[1] A. Acker. Uniqueness and monotonicity of solutions for the interior Bernoulli free boundary problem in the convex n dimensional case. *Nonlinear Anal. Theory Methods Appl.*, 13(12):1409–1425, 1989.

[2] A. Acker and R. Meyer. A free boundary problem for the p-Laplacian: uniqueness, convexity, and successive approximation of solutions. *Electron. J. Differ. Equ.*, 8:1–20, 1995.

[3] P.R.S. Antunes and B. Bogosel. Parametric shape optimization using the support function. arXiv:1809.00254, 2018.

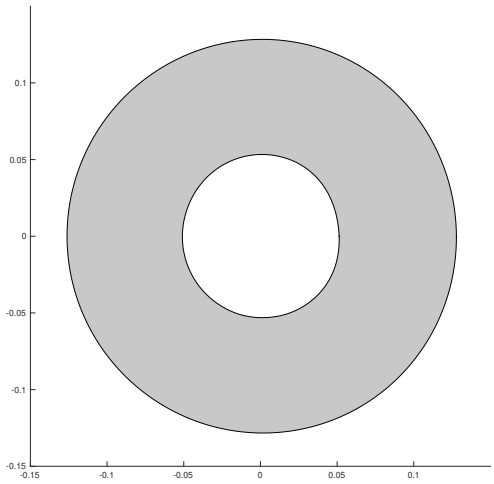

Figure 5: The mean of the support functions of the interior boundary and the exterior boundary in case of the second example.

[4] G. Allaire and C. Dapogny. A linearized approach to worst-case design in parametric and geometric shape optimization. *Math. Models Methods Appl. Sci.*, 24:2199–2257, 2014.

[5] G. Allaire and C. Dapogny A deterministic approximation method in shape optimization under random uncertainties. *SMAI J. Comput. Math.*, 1:83–143, 2015.

[6] A. Beurling. Free boundary problems for the Laplace equations. *Institute for Advanced Study Seminar*, Princeton, NJ, 1957, pages 248–263.

[7] G. Buttazzo and B. Velichkov. A shape optimal control problem with changing sign data. *SIAM J. Math. Anal.*, 50(3):2608–2627, 2018.

[8] C. Choirat and R. Seri. Bootstrap confidence sets for the Aumann mean of a random closed set. *Comput. Stat. Data Anal.*, 71:803–817, 2014.

[9] M. Dambrine, C. Dapogny, and H. Harbrecht. Shape optimization for quadratic functionals and states with random right-hand sides. *SIAM J. Control Optim.*, 53(5):3081–3103, 2015.

[10] M. Dambrine, H. Harbrecht, and B. Puig. Incorporating knowledge on the measurement noise in electrical impedance tomography. *ESAIM: Control Optim. Calc. Var.*, 25:84, 2019.

[11] M. Dambrine, H. Harbrecht, M.D. Peters, and B. Puig, On Bernoulli's free boundary problem with a random boundary. *Int. J. Uncertain. Quantif.*, 7:335–353, 2017.

[12] M. Dambrine and B. Puig Oriented distance point of view on random sets. *ESAIM: Control Optim. Calc. Var.*, 26:84, 2020.

[13] M. Flucher and M. Rumpf. Bernoulli's free-boundary problem, qualitative theory and numerical approximation. *J. Reine Angew. Math.*, 486:165–204, 1997.

[14] H. Harbrecht and G. Mitrou. Improved trial methods for a class of generalized Bernoulli problems. *J. Math. Anal. Appl.*, 420(1):177–194, 2014.

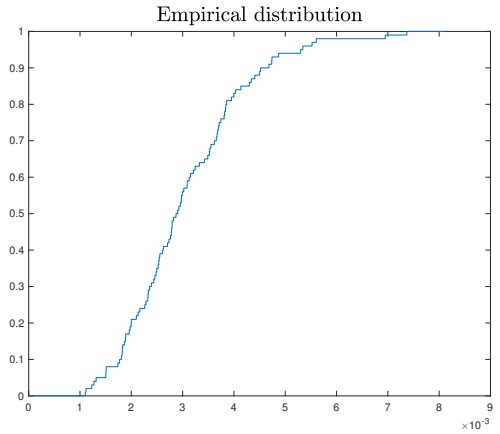

Figure 6: The empirical cumulative distribution $\hat{F}_N$ scaled by the factor $\sqrt{n}$ in case of the second example.

[15] H. Harbrecht and M. Peters. Solution of free boundary problems in the presence of geometric uncertainties. In M. Bergounioux et al., editors, *Topological Optimization and Optimal Transport in the Applied Sciences*, pages 20–39, de Gruyter, Berlin-Bosten, 2017.

[16] M. Hayouni, A. Henrot, and N. Samouh. On the Bernoulli free boundary problem and related shape optimization problems. *Interfaces Free Bound.*, 3:1–13, 2001.

[17] A. Henrot and H. Shahgholian. Convexity of free boundaries with Bernoulli type boundary condition. *Nonlinear Anal. Theory Methods Appl.*, 28(5):815–823, 1997.

[18] H. Jankowski and L. Stanberry, Confidence regions for means of random sets using oriented distance functions. *Scand. J. Stat.*,39:340–357, 2012.

[19] R. Kress. *Linear Integral Equations*. Springer, New York, Third edition, 2014.

[20] R. Kress. On Trefftz's integral equation for the Bernoulli free boundary value problem. *Numer. Math.*, 136:503–522, 2017.

[21] I. Molchanov. *Theory of Random Sets*. Probability and Its Applications, Springer, London, 2005

[22] M.L. Puri and D.A. Ralescu. Limit theorems for random compact sets in Banach space. *Math. Proc. Cambridge Philos. Soc.*, 97(1):151–158, 1985.

[23] R. Schneider. *Convex Bodies: The Brunn-Minkowski Theory*. Vol. 151 of Encyclopedia of Mathematics and its Applications, Cambridge University Press, Cambridge, 2013.

[24] D.E. Tepper. On a free boundary problem, the starlike case. *SIAM J. Math. Anal.*, 6(3):503–505, 1975.

[25] T. Tiihonen and J. Järvinen. On fixed point (trial) methods for free boundary problems. In S.N. Antontsev, A.M. Khludnev, and K.-H. Hoffmann, editors, *Free Boundary Problems in Continuum Mechanics*, volume 106 of *International Series of Numerical Mathematics*, pages 339–350. Birkäuser, Basel, 1992.

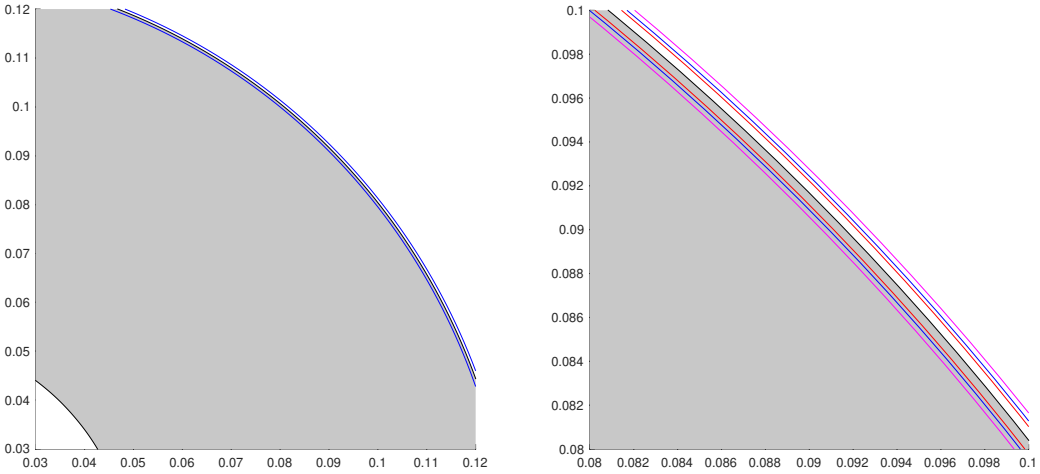

Figure 7: The 95 % asymptotic confidence region for the empirical estimator in case of the second example. Left for $n = 100$. Right for $n = 50, 100$ and 200.

[26] W. Weil. An application of the central limit theorem for Banach-space-valued random variables to the theory of random sets. *Zeitschrift für Wahrscheinlichkeitstheorie und Verwandte Gebiete*, 60(2):203–208, 1982.

[27] O. Ivanyshyn Yaman and R. Kress. Nonlinear integral equations for Bernoulli's free boundary value problem in three dimensions. *Comput Math Appl.*, 74(11):2784–2791, 2017.